Investigation of Drug–Model Cell Membrane Interactions Using Sum Frequency Generation Vibrational Spectroscopy: A Case Study of Chlorpromazine

ARTICLE *in* THE JOURNAL OF PHYSICAL CHEMISTRY C · JULY 2014

Impact Factor: 4.77 · DOI: 10.1021/jp503038m

THE JOURNAL OF PHYSICAL CHEMISTRY C

Article

pubs.acs.org/JPCC

Investigation of Drug–Model Cell Membrane Interactions Using Sum Frequency Generation Vibrational Spectroscopy: A Case Study of Chlorpromazine

Fu-Gen Wu,*[,†,‡] Pei Yang,[‡] Chi Zhang,[‡] Xiaofeng Han,[†,‡] Minghu Song,[§] and Zhan Chen*[,‡]

[†]State Key Laboratory of Bioelectronics, School of Biological Science and Medical Engineering, Southeast University, Nanjing 210096, China

[‡]Department of Chemistry, University of Michigan, 930 North University Avenue, Ann Arbor, Michigan 48109, United States

[§]Compound Safety Prediction Group, Pfizer Inc., Groton, Connecticut 06340, United States

ABSTRACT: Sum frequency generation (SFG) vibrational spectroscopy and attenuated total reflection Fourier transform infrared (ATR-FTIR) spectroscopy were applied to study interactions between an antipsychotic agent, chlorpromazine (CPZ), and model cell membranes consisting of either distearoylphosphatidylcholine (DSPC) or dipalmitoylphosphatidylglycerol (DPPG). The PC and PG lipids represent the zwitterionic and anionic components of the cell membranes, respectively. For an isotopically asymmetric bilayer composed of a deuterated lipid leaflet and a hydrogenated lipid leaflet, the time-dependent SFG signals from the lipids revealed that CPZ can significantly accelerate the flip-flop process of the neutral DSPC bilayer and such an acceleration effect is more pronounced at higher CPZ concentrations. While for the negatively charged DPPG bilayer, it was found that CPZ molecules can immediately bind to and disrupt the outer lipid leaflet and then gradually reduce the ordering of the inner lipid leaflet. A higher CPZ concentration in the subphase leads to a faster disordering effect on the inner leaflet. The association of CPZ to the lipid membranes can be verified by the change in the SFG spectra of the OH stretching vibration of the interfacial water molecules. ATR-FTIR results revealed that addition of CPZ to the subphase did not exert significant effect on the dDSPC/dDSPC bilayer, especially at low CPZ concentrations (<2 mM). It was found that CPZ can cause gel-to-fluid phase transition of the dDPPG/dDPPG bilayer at CPZ concentrations below 2 mM, and higher CPZ concentrations can lead to dissolution of the bilayer. This work demonstrated that SFG (along with ATR-FTIR) is a powerful in situ and label-free technique that can be used to study various aspects of the drug–membrane interactions at the molecular level.

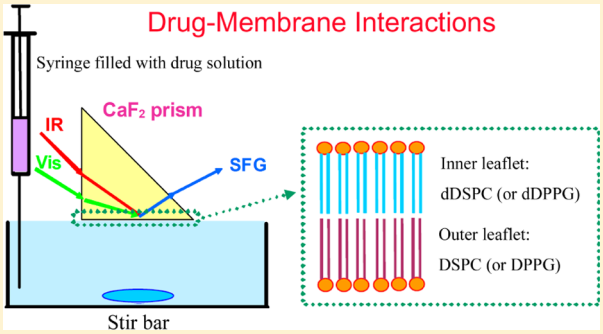

1. INTRODUCTION

Plasma membrane, the boundary between a cell and its surroundings, is the vanguard of the cell to come into contact with drug, nutrient, pathogen, or other molecules in the environment. Many current pharmaceuticals are amphiphilic or catamphiphilic, enabling them to extensively interact with biological membranes. Drug–membrane interaction plays an important role in drug accumulation, distribution, efficacy, and resistance.[1] Understanding various modes of the drug–cell membrane interaction is crucial to develop a better understanding of drug action and for the current and future pharmaceutical research.

Chlorpromazine (CPZ), a phenotiazine with neuroleptic activity, is widely used to treat certain psychiatric disorders. CPZ can extensively interact with cell membranes and proteins, and sometimes it can be used as a local anesthetic. CPZ can also be involved in some membrane-associated cellular processes.[2−4] Similar to many other phenothiazine derivatives, CPZ is amphipathic and can readily bind to and partition into cell membranes. Before reaching their final site of action in the central nervous system, antipsychotics such as CPZ have to permeate through a number of lipid-dominated barriers (e.g., the blood-brain barrier). Therefore, it is important to examine CPZ–membrane interactions.

Experiments carried out to understand the interactions between CPZ and model cell membranes revealed that CPZ effectively interacts with membrane phospholipids, especially with negatively charged ones such as phosphatidylserine (PS)[5−10] and phosphatidylglycerol (PG).[11−14] CPZ, with its pK_a = 9.4,[15] remains mostly protonated and positively charged at the physiological pH. It was reported that neutral CPZ is predominantly found in the hydrophobic tail region, whereas protonated CPZ is located at the lipid–water interface.[16] The partition coefficient of CPZ between the aqueous medium and lecithin bilayer has been accurately measured.[17,18] The adsorption and partition of CPZ to the lipid membrane can

Received: March 27, 2014
Revised: May 26, 2014
Published: July 14, 2014

   dx.doi.org/10.1021/jp503038m | J. Phys. Chem. C 2014, 118, 17538–17548

disrupt the membrane ordering (or increase the membrane fluidity),[19−21] which affects the phase state and phase behavior of the membrane.[5,6,12,22−24] Since the cell membrane regulates molecular transport, cell adhesion, and intercellular signaling, the significant effects exerted by CPZ can thereby change many biological processes that occur at the membrane surface.

In this work, to get a detailed picture of the drug−membrane interaction process at the molecular level, we applied a nonlinear optical spectroscopic technique, sum-frequency generation (SFG) vibrational spectroscopy, and a linear spectroscopic technique, attenuated total reflection Fourier transform infrared (ATR-FTIR) spectroscopy, to study how CPZ interacts with the phospholipid membranes. Nonlinear optical spectroscopic techniques have been used to study the drug−membrane interactions previously. For example, Conboy and co-workers used a novel ultraviolet−visible sum frequency generation (UV−vis SFG) technique to directly detect drug association to lipid membranes without the need for chemical modification.[25] They also reported the use of second harmonic generation (SHG) to image the interactions between the local anesthetic tetracaine and a multicomponent planar substrate supported lipid bilayer array in a label-free manner.[26] Herein, the detailed interaction mechanism between CPZ and lipid membrane was investigated using IR-Vis SFG. 1,2-Distearoyl-*sn*-glycerol-3-phosphocholine (DSPC) and 1,2-dipalmitoyl-*sn*-glycero-3-phospho-(1′-rac-glycerol) (sodium salt) (DPPG) were chosen as model lipids to represent zwitterionic and negatively charged lipid components that are commonly present in biological membranes. Interactions between CPZ at different solution concentrations and the two lipids were investigated and the results revealed that CPZ can significantly accelerate the flip-flop process of the zwitterionic DSPC bilayer. For the negatively charged DPPG bilayer, CPZ molecules can immediately bind to and disrupt the outer lipid leaflet and then gradually destroy the ordering of the inner leaflet.

2. EXPERIMENTAL SECTION

2.1. Sample Preparation. 1,2-Dipalmitoyl-*sn*-glycero-3-phosphocholine (DPPC), 1,2-dipalmitoyl(d_{62})-*sn*-glycero-3-phosphocholine (dDPPC), 1,2-dipalmitoyl-*sn*-glycero-3-phospho-(1′-rac-glycerol) (sodium salt) (DPPG), 1,2-dipalmitoyl-(d_{62})-*sn*-glycero-3-phospho-(1′-rac-glycerol) (sodium salt) (dDPPG), 1,2-distearoyl-*sn*-glycerol-3-phosphocholine (DSPC), and 1,2-distearoyl(d_{70})-*sn*-glycero-3-phosphocholine (dDSPC) were purchased from Avanti Polar Lipids. The purity of all these phospholipids is higher than 99%. CPZ hydrochloride (purity ≥98%) was purchased from Sigma-Aldrich. The molecular formulas of these lipid molecules and CPZ are shown in Figure 1.

Right-angle CaF_2 prisms were purchased from Chengdu YaSi Opteoelectronics Co, Ltd. (Chengdu, China). The CaF_2 prisms were soaked in toluene overnight and then washed with Contrex AP detergent solution from Decon Laboratories (King of Prussia, PA). After that, they were rinsed with copious amounts of deionized water and then dried in nitrogen. The prisms were further oxygen plasma treated for 3 min immediately before the lipid deposition. The Langmuir−Blodgett and Langmuir−Schaefer (LB/LS) methods were used to deposit the proximal (inner) and the distal (outer) leaflets of a single lipid bilayer onto a prism, respectively. A KSV2000 LB system and ultrapure water (18.2 MΩ cm) from a Millipore system (Millipore, Bedford, MA) were used for the bilayer preparation. Briefly, a prism was attached to a sample

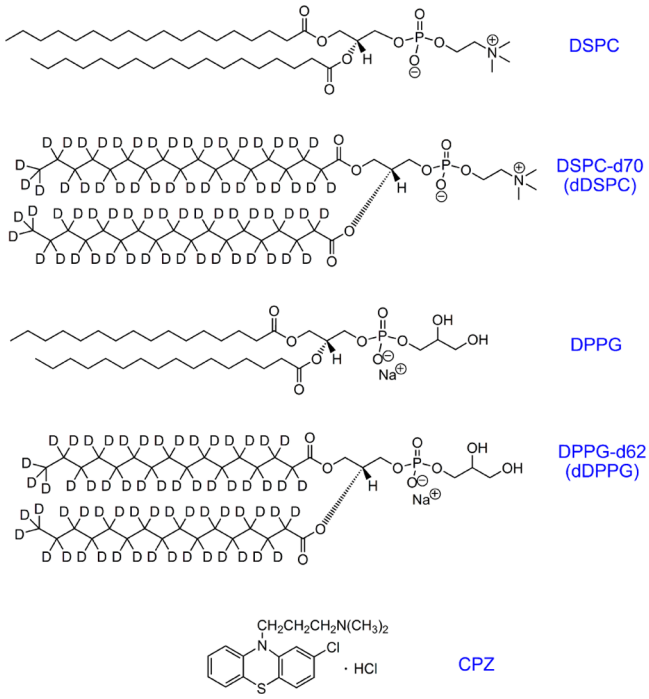

Figure 1. Molecular formulas of DSPC, dDSPC, DPPG, dDPPG, and CPZ.

holder via one right-angle face so that the other right-angle face was perpendicularly immersed in the water inside the Langmuir trough. An appropriate amount of lipid chloroform solution was then gently spread onto the water surface, and the chloroform was allowed to evaporate for at least 10 min. The monolayer area was compressed by two barriers at a rate of 5 mm/min until a surface pressure of 34 mN/m was reached. The prism was lifted out of the subphase at a rate of 1 mm/min. After that, the monolayer deposited CaF_2 prism was fixed on the sample holder in the SFG sample stage. After adjusting and maximizing the SFG signal from the CD stretching vibration of the deuterated lipid components (Input laser beams were incident onto one of the right-angle faces of a prism and then reflected by the other right-angle face coated with the lipid monolayer or bilayer, as shown in Figure 2.), we started to collect the time-dependent SFG signals at two wavenumbers of 2070 cm^{-1} (CD_3 symmetric stretching vibration in deuterated phospholipid) and 2875 cm^{-1} (CH_3 symmetric stretching vibration in hydrogenated phospholipid).

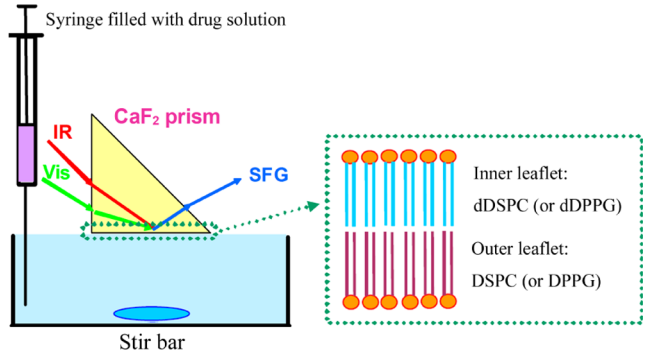

Figure 2. SFG experimental sample geometry to study drug−model cell membrane interactions.

dx.doi.org/10.1021/jp503038m | J. Phys. Chem. C 2014, 118, 17538−17548

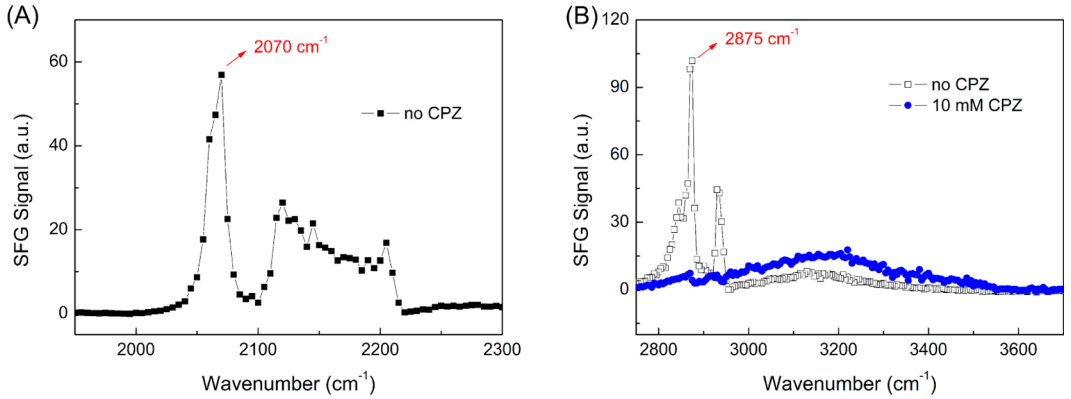

Figure 3. SFG spectra of the dDSPC/DSPC bilayer collected in the frequency regions of (A) 1950−2300 and (B) 2750−3700 cm^{-1}. SFG spectrum collected after the addition of 10.0 mM CPZ solution to the bilayer subphase is also shown in part B in blue.

After that, a 20 mL plastic dish filled with Millipore water was placed on a height-adjustable stage, just below the prism. A monolayer of lipid at the surface pressure of 34 mN/m was prepared by spreading one or two drops of lipid chloroform solution. Since it is difficult to control exactly a surface pressure at 34 mN/m, in our experiment, after adding one or two drops of 1 mg/mL lipid/chloroform solution onto the water surface, if the surface pressure exceeds 34 mN/m, we used an Eppendorf pipet tip to contact with the surface to remove some lipids from the surface, making the surface pressure exactly at 34 mN/m. After evaporation of chloroform, the stage was slowly lifted until the water surface contacted with the prism surface to form a lipid bilayer. At 60 s after the formation of the bilayer, CPZ stock solution was injected into the subphase using a Hamilton syringe. The subphase was stirred using a magnetic stir bar at the bottom of the plastic dish to ensure the homogeneity of the suhphase. The time-dependent SFG signals were collected from the lipid monolayer on prism before the contact and from bilayer after the contact. All experiments were carried out at room temperature (22 °C), at which the studied lipid molecules were all in the gel phase. The prism was arranged so that the total reflection for the 532 nm green beam was just achieved.

2.2. SFG Introduction. SFG is a second-order nonlinear optical spectroscopic technique that has submonolayer surface sensitivity.[27,28] This surface sensitivity makes SFG an ideal technique to monitor the reorientation process of submonolayer molecules in situ. The details regarding SFG theories and measurements have been published previously,[29−48] and will not be repeated here. The SFG setup used in this study was a ps-SFG system purchased from EKSPLA. In our experiments, two laser beams (a 532 nm visible and a frequency-tunable infrared) were overlapped in space and time on the sample, generating a signal at the sum frequency ($\omega_{vis} + \omega_{IR} = \omega_{sum}$). The IR beam tunable between 2.5 and 10 μm (with a line width <6 cm^{-1}) is obtained from an optical parametric generation/amplification/difference frequency generation (OPG/OPA/DFG) system based on LBO and $AgGaS_2$ crystals, which were pumped by the third harmonic and the fundamental output of the laser. Both beams had a pulse width of 20 ps and a repetition rate of 20 Hz. The pulse energies of both input beams were around 100 μJ, and the beam sizes were around 500 μm. By controlling the polarizations of the input and generated signal beams, information on the interfacial molecular orientation can be obtained. All of the spectra presented in this work were collected using ssp (s-polarized output SFG signal, s-polarized input visible beam, and p-polarized input IR beam, respectively) polarization combination. All the SFG signals were normalized to compensate the IR and visible beam power fluctuations.

2.3. SFG Data Analysis. The SFG signal intensity (I) is proportional to the square of the effective second order nonlinear optical susceptibility $\chi^{(2)}_{eff}$, which depends on the IR frequency:[27,28]

$$I \propto |\chi^{(2)}_{eff}|^2 \tag{1}$$

$$\chi^{(2)}_{eff} \propto \chi^{(2)}_{NR} + \sum_q \frac{A_q}{\omega_q - \omega_{IR} - i\Gamma_q} \tag{2}$$

where $\chi^{(2)}_{NR}$ represents the nonresonant susceptibility, A_q is the signal strength, ω_q and ω_{IR} represent the frequencies of the vibrational transition and the infrared beam respectively, and Γ_q is the damping coefficient.

The intensity of the SFG signal contributed by the CH_3 (or CD_3) symmetric stretching vibration is proportional to the net population difference for the hydrogenated (or deuterated when calculating the CD_3 signal) lipid species in the two leaflets and can be expressed as[49−51]

$$I_{CH_3 or CD_3} \propto (N_{inner} - N_{outer})^2 \tag{3}$$

where N_{inner} and N_{outer} respresent the number of lipids in the inner leaflet and outer leaflet, respectively. At the time when the upper layer contacted with the lower layer to form an isotopically asymmetric bilayer, the SFG signal should have the largest value. As time went by, the net population difference of the hydrogenated (or deuterated) lipids decreased (e.g., due to flip-flop), resulting in the decrease in I_{CH_3} (or I_{CD_3}).

As has been demonstrated by Conboy and co-workers, the lipid flip-flop kinetics can be investigated by fitting the SFG time-dependent signal using the following single exponential function:[49,52−54]

$$I_{CH_3 or CD_3}(t) = I_{max} e^{-4kt} + I_{min} \tag{4}$$

where I_{max} and I_{min} are the maximum and minimum resonant SFG signal intensities from CH_3 or CD_3 symmetric stretching modes in lipid alkyl chain, respectively; k is the flip-flop rate. Besides, the half-life ($t_{1/2}$) of lipid flip-flop in terms of the population inversion can also be calculated by the above determined k value:[52]

dx.doi.org/10.1021/jp503038m | J. Phys. Chem. C 2014, 118, 17538−17548

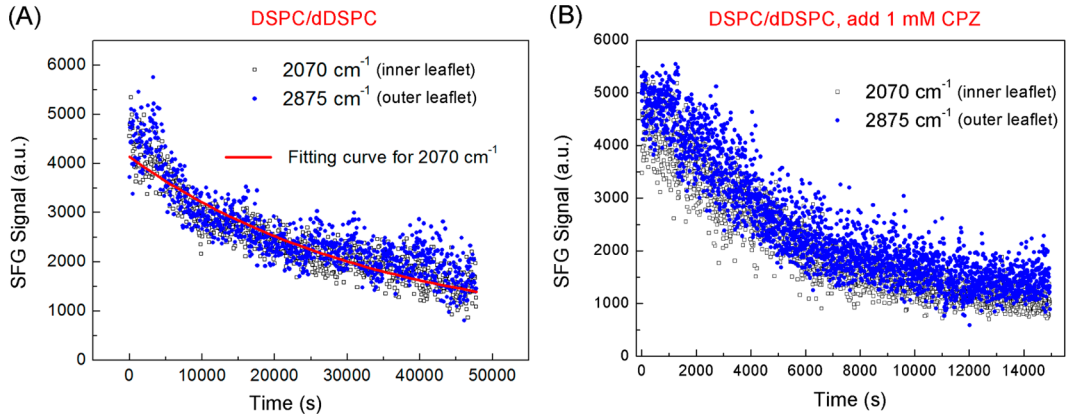

Figure 4. (A) Time-dependent SFG signals at 2070 and 2875 cm^{-1} detected from the dDSPC/DSPC bilayer. The red line is the fitting result for the 2070 cm^{-1} signal using eq 4. (B) Time-dependent SFG signals collected at 2070 and 2875 cm^{-1} from the dDSPC/DSPC bilayer after the addition of 1.0 mM CPZ to the subphase.

$$t_{1/2} = \frac{\ln 2}{2k} \quad (5)$$

which is based on a value of total population inversion of 0.5.

2.4. ATR-FTIR Experiment. The dDSPC/dDSPC and dDPPG/dDPPG bilayers were prepared on the clean ATR-FTIR ZnSe crystal (Specac, U.K.) surfaces for ATR-FTIR experiments by using LB/LS method as mentioned above. The ZnSe crystal was washed extensively with detergent, ethanol, and water, and was oxygen plasma treated for 2 min immediately before the lipid deposition to make the surface hydrophilic. The IR spectra were collected using a Nicolet iS50 spectrometer with the ATR accessory. All spectra presented were averaged over 32 scans. After collecting the spectra from the neat lipid bilayer (dDSPC/dDSPC or dDPPG/dDPPG) in contact with water, a CPZ stock solution was added to the ATR cell to reach a certain concentration of CPZ (0.1 mM to 10.0 mM). Spectra were collected from the lipid bilayer 10 min after the addition of CPZ. All ATR-FTIR experiments were also carried out at room temperature (22 °C).

3. RESULTS AND DISCUSSION

3.1. Interaction of CPZ with Zwitterionic DSPC and DPPC Bilayers. Figure 3 shows the SFG spectra of the dDSPC/DSPC (proximal/distal leaflet, or inner/outer leaflet) bilayer collected immediately after the contact of the two lipid monolayers to form the lipid bilayer. The signals detected in the C−D stretching frequency regime (2000−2300 cm^{-1}) and the C−H stretching frequency regime (2750−3100 cm^{-1}) probe the inner and outer leaflets of the lipid bilayer, respectively. The peak at 2070 cm^{-1} is from the CD_3 symmetric stretching mode. The broad feature covers between 2100 and 2220 cm^{-1} contains the CD_2 symmetric stretching mode (~2120 cm^{-1}), CD_3 asymmetric stretching mode (~2200 cm^{-1}), and possibly other CD stretching modes as well. The peaks at 2875 and 2940 cm^{-1} come from the CH_3 symmetric stretching mode and the CH_3 Fermi resonance, respectively.[34] The broad peaks centered at around 3180 and 3400 cm^{-1} originate from the OH stretching modes of interfacial water molecules that are aligned by the surface charges.[34] The initial isotopically asymmetric bilayer formed immediately after the contact of the two monolayers had the largest net population difference of the hydrogenated (or deuterated) lipid species in the two leaflets. As time went by, the transbilayer movement (flip-flop) of the lipid molecules within the bilayer led to the decrease in the net population difference of the hydrogenated (or deuterated) lipids between the two leaflets, resulting in the decrease of I_{CH_3} (or I_{CD_3}). Figure 4A shows the change of SFG signal with time for the neat dDSPC/DSPC bilayer. The changes in the SFG signals at 2070 and 2875 cm^{-1} are simultaneous and the time-dependent signal can be fitted with a single exponential function (eq 4). The deduced flip-flop rate (k) and half-life ($t_{1/2}$) are listed in Table 1. We should point out that the value k on a specific solid substrate (window or prism) depends strongly on temperature and the surface charge (e.g., silica is slightly negatively charged while CaF_2 is slightly positively charged) and roughness of the solid substrate. Thus, to obtain repeatable kinetic results, we used the same type of CaF_2 prisms from the same purchase order for the flip-flop study.

Table 1. Kinetics of SFG Signal Decrease of the dDSPC/DSPC Bilayer and the Inner Leaflet of the dDPPG/DPPG Bilayer at 22 °C as a Function of the Concentration of CPZ Solution in Contact with the Bilayers[a]

	dDSPC/DSPC		dDPPG/DPPG
C_{CPZ} (mM)	k (s^{-1})	$t_{1/2}$(s)	t_{end} (s)
0	7.3×10^{-6}	4.7×10^{4}	$>4.0 \times 10^{4}$
0.1	7.9×10^{-6}	4.4×10^{4}	1.3×10^{4}
0.2	1.2×10^{-5}	2.9×10^{4}	5.8×10^{3}
0.5	3.0×10^{-5}	1.2×10^{4}	1.2×10^{3}
1.0	6.0×10^{-5}	5.8×10^{3}	4.0×10^{2}
2.0	9.7×10^{-5}	3.6×10^{3}	2.0×10^{2}
5.0	2.2×10^{-4}	1.6×10^{3}	1.5×10^{2}
10.0	5.9×10^{-4}	5.9×10^{2}	1.0×10^{2}

[a] k = filp-flop rate constant; $t_{1/2}$ = the time required for the SFG signal intensity to decrease by 50%; t_{end} = the time required for the SFG signal to decrease to I_{min}. The errors are estimated to be less than 20%.

Shown in Figure 4B is a typical example of the time-dependent SFG signal decrease caused by the interaction between CPZ (1.0 mM in solution) and the dDSPC/DSPC bilayer. The time-dependent SFG signal decrease was caused by the decrease in the asymmetrical distribution of the two isotopically different lipid species in the two leaflets, or by the disruption effect caused by the insertion of CPZ molecules into the bilayer, or by both. Figure 4B shows that the time-

dx.doi.org/10.1021/jp503038m | J. Phys. Chem. C 2014, 118, 17538−17548

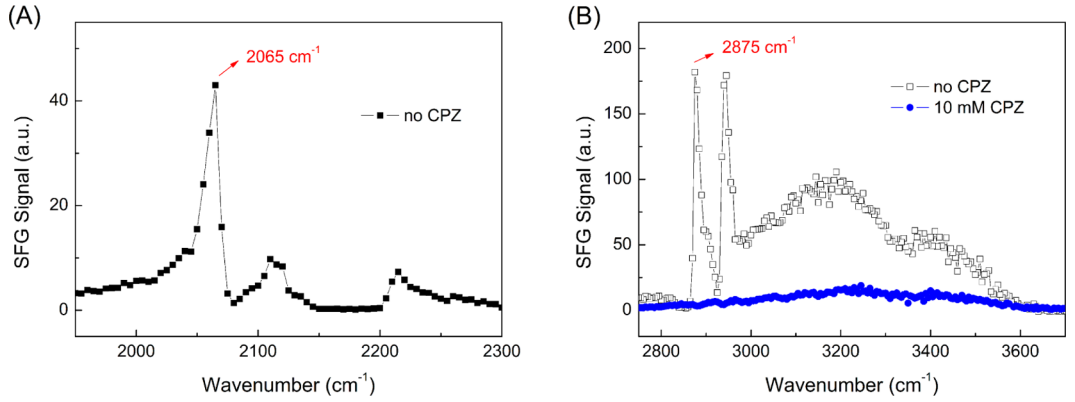

Figure 5. SFG spectra collected from the dDPPG/DPPG bilayer in the frequency regions of (A) 1950−2300 and (B) 2750−3700 cm^{-1}. SFG spectrum collected after the addition of 10.0 mM CPZ solution to the subphase in contact with the bilayer is also shown in part B in blue.

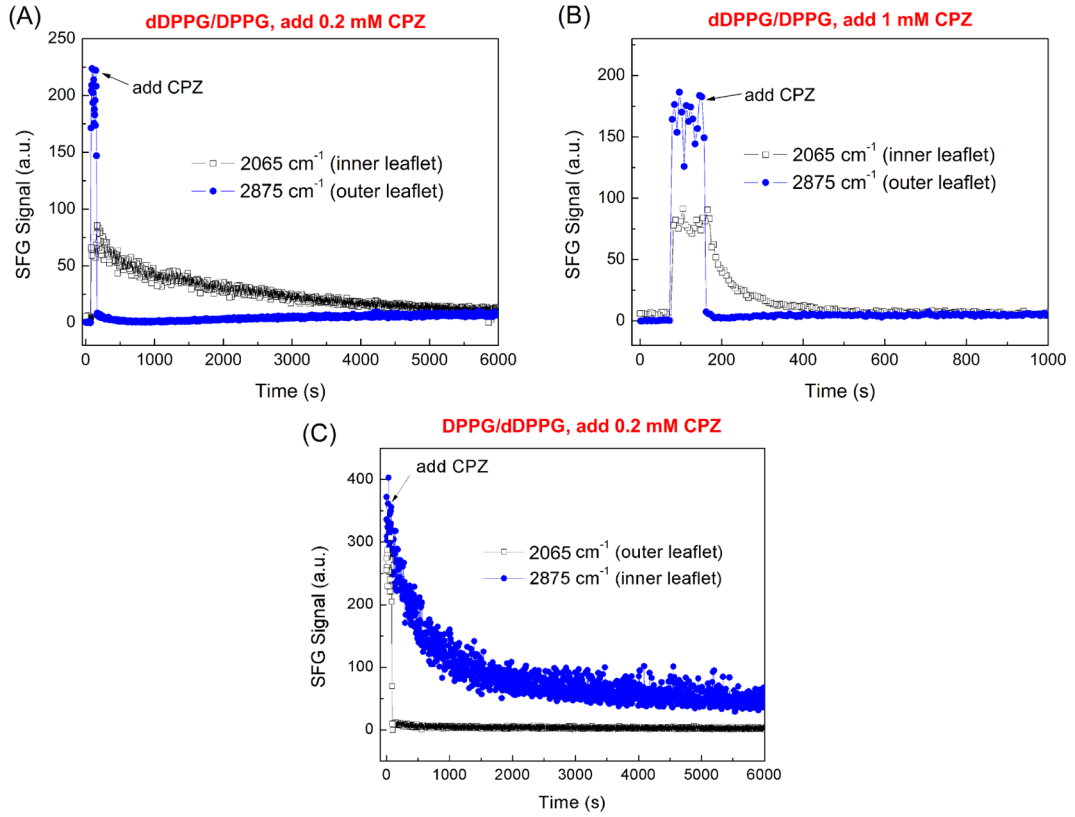

Figure 6. Time-dependent SFG signals detected at 2065 and 2875 cm^{-1} from the dDPPG/DPPG bilayer after the addition of 0.2 mM CPZ solution (A) and 1 mM CPZ solution (B) to the subphase. The time-dependent SFG signals detected for DPPG/dDPPG after the addition of 0.2 mM CPZ was also shown in part C.

dependent SFG signal decreases for the two leaflets have very similar rates, indicating that the changes of the two leaflets have very similar dynamics, which is a strong evidence to support the occurrence of the flip-flop process.

We also studied the concentration effects of CPZ in the subphase on the flip-flop kinetics of the lipid bilayers and the results are summarized in Table 1. It can be seen that the higher the concentration of the drug was, the larger the transbilayer rate was measured. Besides, only when the concentration of CPZ was above 0.2 mM, could the flip-flop kinetics be significantly affected. After the addition of the CPZ stock solution to the subphase, CPZ molecules can be adsorbed onto the interfacial region of the outer leaflet of the bilayer, resulting in a disordered packing of the lipid molecules in the outer leaflet. The specific binding of CPZ to the interfacial region of PC molecules has been reported. The charged amine group in CPZ interacts with the PC phosphate region, while the CPZ tricyclic ring inserts into the lipid bilayer which affects mostly the properties of the carbonyl and first methylene groups of the lipid.[55] Besides, CPZ molecules may also move from the outer layer to the inner layer, which may subsequently loosen the packing of the lipid molecules in the inner leaflet and further accelerate the flip-flop. Therefore, the lipid transbilayer movement or lipid flip-flop in the dDSPC/DSPC bilayer was significantly accelerated compared to the lipid bilayer without CPZ in the subphase. Perhaps the initial adsorption and moving process of CPZ was very fast, or in this process the flip-

dx.doi.org/10.1021/jp503038m | J. Phys. Chem. C 2014, 118, 17538−17548

flop already occurred, therefore we observed that the SFG signal decrease rates for the two leaflets were almost identical.

In addition to the dDSPC/DSPC bilayer, we have also investigated the effect of the addition of CPZ to the subphase on the flip-flop rate of a different lipid bilayer, the dDPPC/DPPC bilayer. The flip-flop rate of the dDPPC/DPPC bilayer is faster than the dDSPC/DSPC bilayer. Similar to the interactions between CPZ and the dDSPC/DSPC bilayer discussed above, the SFG results revealed that the flip-flop rate for the system after the addition of CPZ ($k = 1.2 \times 10^{-3}$ s^{-1}) to the subphase (to reach 1.0 mM) of the dDPPC/DPPC bilayer was significantly larger than that for the neat lipid bilayer system ($k = 1.4 \times 10^{-4}$ s^{-1}). The above results indicate CPZ can exert similar membrane interaction effect on DSPC and DPPC bilayers through inducing lipid transbilayer movements or flip-flop.

3.2. Interaction of CPZ with DPPG Bilayers. Figure 5 shows the SFG spectra of a dDPPG/DPPG bilayer collected immediately after the formation of the lipid bilayer. Similar to the dDSPC/DSPC bilayer system, the peak at 2065 cm^{-1} comes from the CD_3 symmetric stretching vibration and the 2875 cm^{-1} signal comes from the CH_3 symmetric stretching vibration. These two peaks can be used to probe the molecular changes of the inner and outer lipid leaflets, respectively.

Figure 6 displays the time-dependent SFG signal change during the interaction between CPZ and the dDPPG/DPPG or DPPG/dDPPG bilayer. We can see that before the contact of the two lipid leaflets, only weak CD stretching vibrational signal contributed from the dDPPG monolayer in air was detected (for a clearer SFG signal before the formation of lipid bilayer, see Figure 6B). When the dDPPG monolayer on the prism contacted with the DPPG monolayer spread on water, a lipid bilayer was formed. The significant increase of the SFG intensity of the CH_3 and CD_3 stretching vibrations upon contacting with water is mainly due to the change of Fresnel factors and will be discussed in detail elsewhere. After the addition of CPZ stock solution to the subphase (to reach 0.2 mM), the CH_3 symmetric stretching signal contributed from the outer DPPG layer immediately decreased to zero, while the CD_3 symmetric stretching signal contributed from the inner dDPPG layer decreased gradually and reached equilibrium (around 0) after ~1.6 h (Figure 6A). We have also investigated the addition of CPZ to the subphase (to reach 0.2 mM) of a DPPG/dDPPG bilayer (where the inner and outer leaflets were switched from the dDPPG/DPPG bilayer examined above) and the result is shown in Figure 6C. Similarly, after the addition of CPZ to the subphase, the CD_3 symmetric stretching signal (contributed from the outer dDPPG layer) immediately decreased to zero. These results revealed that for DPPG bilayers, the outer and the inner leaflets have very different signal decrease dynamics while interacting with CPZ.

We increased the concentration of CPZ in the subphase and then studied the membrane−CPZ interaction. For 1.0 mM CPZ in the subphase of the dDPPG/DPPG bilayer, the SFG signal of CH_3 symmetric stretching mode coming from the outer DPPG leaflet also immediately decreased to zero after the addition of CPZ (Figure 6B), as in the case of 0.2 mM CPZ. However, the CD_3 symmetric stretching signal contributed from the inner lipid layer dropped faster than the 0.2 mM CPZ case, decreasing to zero after ~7 min. The immediate drop of the CH_3 symmetric stretching signal from the outer DPPG leaflet upon the addition of CPZ to the subphase was observed for all the CPZ concentrations ranging from 0.1 to 10.0 mM.

The pH values of the CPZ solutions with different concentrations were measured to be 8.0 for 0.1 mM, 7.6 for 0.2 mM, 7.0 for 0.5 mM, 6.8 for 1.0 mM, 6.6 for 2.0 mM, 5.8 for 5.0 mM, and 5.6 for 10.0 mM. Since CPZ has a pK_a value around 9.4, the CPZ molecules in all the above solutions are positively charged. Thus, when the positively charged CPZ molecules interact with the negatively charged DPPG bilayer, they immediately bind to the PO_4^- groups in the lipid polar region through the strong electrostatic (attractive) interaction. This facilitates the immediate strong interaction between the hydrophobic tricyclic ring of CPZ and the lipid hydrocarbon chains. Such a strong interaction immediately disrupts the lipid outer leaflet thus the SFG signal contributed from the outer leaflet dropped to zero quickly. The binding of CPZ with the outer leaflet of DPPG may not be static and the CPZ molecules may move to the inner leaflet. We believe that the movement of CPZ from the outer leaflet to the inner leaflet was not instantaneously. This was reflected by the gradual decrease of the CD_3 symmetric stretching signal contributed from the inner leaflet. The effect of drug concentration on the change of the inner dDPPG leaflet SFG signal was also investigated, and the corresponding results are summarized in Table 1. The results suggest that the higher the concentration of CPZ was, the faster the disordering of the inner lipid leaflet occurred.

3.3. Comparison between PC and PG Bilayers Interacting with CPZ. We did not observe any SFG signal from CPZ, possibly because of its random orientation in the lipid bilayer. Besides the CH or CD stretching signals especially those from the terminal CH_3 or CD_3 groups in the lipid tails, we can also derive some important information from the OH stretching vibration of the interfacial water molecules. In the lipid−water interfacial region, the water molecules can be aligned by the static electric field, resulting in well orientated water molecules which break the inversion symmetry. Through probing the OH stretching vibration modes of water, SFG spectroscopy can be used to monitor the local water environment.[56] Water at a charged surface can be ordered through the alignment of the water dipoles by the surface electric field.[31,32,39,57−59] The adsorption of charged molecules at a neutral lipid interface would generate an electric field and the adsorption of positively charged molecules would screen the negatively charged lipid headgroups. Both cases will affect the interfacial water structure. Thus, the investigation of the interfacial water structure using SFG can supplement to depict a clear picture of drug−membrane interactions.

We collected SFG spectra (Figures 3B and 5B) in the OH stretching frequency region before and after the CPZ−lipid bilayer interaction. The presence of the peak at 3150 cm^{-1} detected from the zwitterionic dDSPC/DSPC bilayer shows that the interfacial water molecules are ordered at this bilayer interface before the introduction of CPZ to the subphase. The addition of CPZ to the dDSPC/DSPC bilayer subphase (to reach 10 mM) further increased the water signal at around 3150−3170 cm^{-1} (Figure 3B), indicating that the preferential alignment of water molecules at the lipid−water interface was enhanced by the electric field generated by the adsorbed charged drug molecules on the lipid surface.

From the dDPPG/DPPG bilayer, two broad peaks centered at around 3200 and 3400 cm^{-1} (Figure 5B) were observed before the introduction of CPZ. These two peaks can be assigned to the OH stretching modes of hydrogen bonded interfacial water molecules.[60,61] The difference of the SFG water spectra collected from the dDSPC/DSPC and dDPPG/

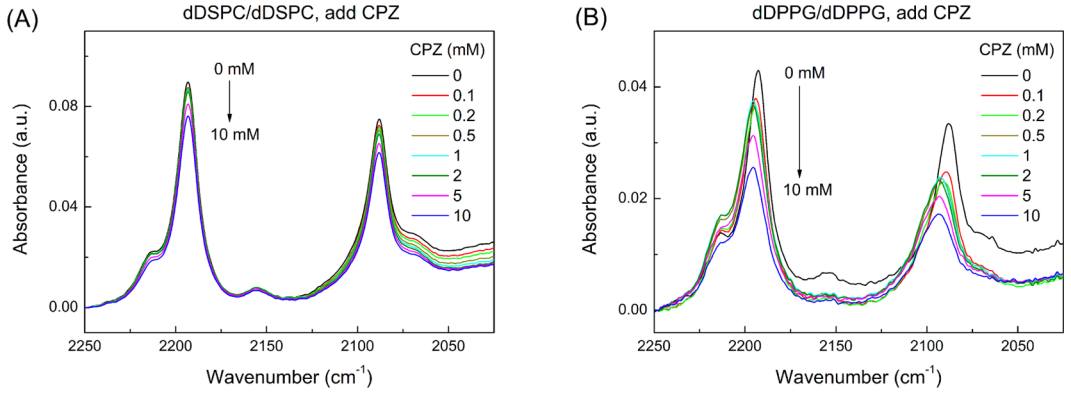

Figure 7. ATR-FTIR spectra of the CD stretching vibrations collected from (A) dDSPC/dDSPC bilayer and (B) dDPPG/dDPPG bilayer after the addition of various CPZ stock solutions to the subphase.

DPPG bilayers reflects different interfacial water environments: The ordered water molecules associated with the dDSPC/DSPC bilayer reside in the region between cationic and anionic parts of the headgroup, while ordered water molecules in dDPPG/DPPG bilayer mainly orient at the charged lipid surface.[36,59] After the addition of CPZ stock solution to the subphase of the dDPPG/DPPG bilayer to reach 10.0 mM CPZ, the water signal centered around 3200 and 3400 cm^{-1} significantly decreased. The electric charges of the negatively charged lipid surface were screened by the oppositely charged drug molecules and the orientation order of water at the lipid−CPZ solution interface therefore decreased substantially. Thus, from the changes in the SFG spectra collected in the OH stretching frequency region of the interfacial water molecules associated with the dDSPC/DSPC and dDPPG/DPPG bilayers, we demonstrated that CPZ molecules indeed bind and partition into both kinds of lipid membranes. This result is consistent with the conclusion drawn by Pickholz, M. et al. that there are specific interactions (hydrogen bonds) between protonated CPZ and the lipid head groups for both zwitterionic and anionic monolayers.[16]

The contrasting SFG results of the PC and PG bilayers interacting with CPZ strongly suggest that there are two different interaction modes between CPZ and the lipid molecules bearing different headgroup structures. Evidence from previous monolayer studies revealed that the addition of micromolar concentrations of CPZ can cause a significant expansion of the mean molecular area of the negatively charged phospholipids, but not the neutral glycerophospholipids.[7,8,62,63] Similar conclusions have also been drawn for bilayer samples (liposomes).[5,10,64,65] For the neutral PCs, it has been reported that only the neutral CPZ molecules can be inserted into the lipid bilayer, locating at the hydrophobic tail region, while the protonated CPZ molecules may reside at the lipid−water interface.[16] As a result, the net CPZ concentration within the bilayer is low due to the partial insertion of the CPZ species into the bilayer. The expansion effect caused by the intercalation of the neutral CPZ can thereby not affect the packing density significantly. Besides, the effects of the neutral CPZ molecules on the two lipid leaflets seem equal as revealed by our time-dependent SFG signals (Figure 4), which may suggest that the packing states of the two leaflets are governed by the neutral form of CPZ. In contrast, the expansion of the lipid film caused by the intercalation of CPZ molecules is more pronounced for the oppositely charged PG molecules due to the electrostatic attraction interaction between the drug molecules and the lipid bilayer. The strong insertion and expansion effect on the PG bilayer significantly increases the mean molecular area of the lipid monolayer, resulting in a loosely and unordered packing of the lipid molecules, which may account for the disappearance of the SFG methyl stretching signal after the addition of the drug molecules. Moreover, the CPZ molecules can further lead to the dissolution (as with most surfactants) of the PGs, as will be demonstrated by our ATR-FTIR results shown below.

Since PG is negatively charged while PC contains no net charge, the interactions between positively charged CPZ and DPPG should be much stronger than that between CPZ and DSPC. Due to this strong interaction, CPZ disrupted the outer leaflet of the dDPPG/DPPG bilayer immediately. Also due to the strong interaction between the outer leaflet and CPZ, it took some time for CPZ to move inside the bilayer and interact with the inner leaflet. Meanwhile, for PC bilayers, the behavior of CPZ is similar to cholesterol. A very recent study revealed that in the cholesterol−PC system, the flip-flop of cholesterol itself is much faster than the phospholipid molecules.[51] For CPZ−PC system, the CPZ molecules added in the subphase can immediately partition into the outer monolayer within several minutes,[18] and since the binding of CPZ to PC molecules is not very strong, the CPZ in the outer monolayer may easily translocate into the inner monolayer (as CPZ leaves the outer monolayer due to translocation into the inner leaflet, some additional CPZ molecules may continuously insert into the outer monolayer), which finally results in a bilayer with the CPZ molecules evenly distributed in both of the two PC leaflets. The translocation of CPZ in the two leaflets of a PC bilayer has been confirmed by isothermal titration calorimetry (ITC) result in a previous work.[18] The lipid disordering effect caused by the distribution of CPZ in one or two leaflets can both accelerate the flip-flop processes of lipids.

Furthermore, one must take into account the critical micellar concentration (CMC) of CPZ (the CMC value of CPZ varied from 0.01 to 1.0 mM in the literature[11]) in the interpretation of the interaction mechanism between CPZ and membrane, since CPZ beyond a given concentration (0.01−1.0 mM) can behave as a detergent.[11] It was found that at very high CPZ concentrations (e.g., well above its CMC), the membrane lipids could be completely dissolved by CPZ due to the formation of mixed micelles, while at lower concentrations membrane leakage and loss of lipid asymmetry were increased.[66−68] However, for all the CPZ concentrations investigated (0.1−10.0 mM), the lipid molecules in the two

dx.doi.org/10.1021/jp503038m | J. Phys. Chem. C 2014, 118, 17538−17548

lipid leaflets of the dDSPC/DSPC bilayer always had the same transbilayer movement rates, indicating that very likely the flip-flop process occurred at all the CPZ concentrations up to 10.0 mM. This shows that the membrane is not completely dissolved even at this highest concentration. For the dDPPG/DPPG bilayer, we found that after the addition of 10.0 mM CPZ, the water signal is still much higher than that of the bare CaF_2 prism in contact with pure water or the bare CaF_2 prism in contact with a 10.0 mM CPZ solution, indicating that there are still lipid molecules on the surface of the prism and the bilayer is not completely dissolved.

To check whether the high concentration CPZ solutions can dissolve the lipid bilayer attached on the solid substrate, ATR-FTIR studies were performed and the deuterated lipid bilayers (dDSPC/dDSPC or dDPPG/dDPPG) used in the ATR-FTIR experiments were constructed using the same method (LB/LS) as those used in the SFG experiment. We can see that after the addition of 0.1−2.0 mM CPZ to the dDSPC/dDSPC bilayer subphase (Figure 7A), the intensity of the ATR-FTIR CD_2 asymmetric stretching vibration (located at 2193 cm^{-1}) only decreased slightly (less than 5%). At the CPZ concentrations of 5.0 mM and 10.0 mM, the lipid CD signal at 2193 cm^{-1} decreased by 10% and 16%, respectively. For the CD_2 symmetric stretching vibration signal (located at 2088 cm^{-1}), similar changes were observed after the lipid bilayers contacting with the CPZ solutions with different concentrations. However, since the feature of the 2088 cm^{-1} peak is significantly affected by the shift of the baselines at the right side of the peak, we did not quantify the peak intensity change. Besides, no peak position change was observed for these two peaks. These results show that the dDSPC/dDSPC bilayer does not have substantial change in its packing state after contacting CPZ solutions, and the dissolution/displacement of the lipids by CPZ is not significant, especially at low CPZ concentrations (<2 mM). For the dDPPG/dDPPG bialyer (Figure 7B), after the addition of 0.1 mM CPZ to the subphase, the peak shape of CD_2 asymmetric and symmetric stretching ATR-FTIR signals located at 2193 and 2088 cm^{-1} experienced significant changes, and the peak positions gradually shift to 2196 and 2093 cm^{-1} at CPZ concentration of 2.0 mM. The blue shift of the peak center and the increase in peak width suggest a gel-to-fluid phase transition of the lipid bilayer:[69] When the CPZ solution concentration increased from 0 to 2.0 mM, the packing of the dDPPG molecules became gradually less ordered, and therefore the phase state of the dDPPG bilayer changed from gel (before the addition of CPZ) to fluid phase (at CPZ concentration of 2.0 mM). To demonstrate that the dDPPG bilayer phase changed from gel to fluid, FTIR experiments were carried out to study dDPPG aqueous dispersion (vesicles) at 20 and 50 °C (dDPPG has a gel to fluid phase transition temperature of 36 °C[70]). The results showed that the CD asymmetric and symmetric stretching signals of the gel-state dDPPG peaked at 2193 and 2089 cm^{-1} at 20 °C, respectively. These two peaks shifted to 2196 cm^{-1} and 2094^{-1} for the fluid phase DPPG at 50 °C. As we presented above, in the ATR-FTIR experiment on the dDPPG bilayer, the CD asymmetric and symmetric stretching signals of the original gel-state bilayer (before the addition of CPZ) peaked at 2193 and 2088 cm^{-1}, respectively; while they shifted to 2196 and 2093 cm^{-1} while in contact with 2.0 mM CPZ solution. This observation is very similar to the heating-induced phase transition of the dDPPG dispersions. This proves that CPZ molecules disrupted the initial ordered packing state of dDPPG/dDPPG bilayer, resulting in the gel-to-fluid phase transition. For the CPZ solution concentrations of 5.0 and 10.0 mM, the ATR-FTIR peaks at 2196 cm^{-1} and 2094^{-1} further decreased in intensity, but the peak positions remained unchanged. Very likely this was caused by the dissolution of dDPPG molecules into the CPZ solution (e.g., forming micelles). The dDPPG/dDPPG bilayer's gel−fluid phase transition at low CPZ concentrations (0 and 2.0 mM) and the dissolution of the dDPPG molecules into the solution at high CPZ concentrations (>2.0 mM) are well correlated to the observed SFG results (shown in Table 1) that the addition of CPZ can accelerate the flip-flop rate of dDPPG/DPPG bilayer: The gel-to-fluid phase change and the dissolution of dDPPG molecules either from the outer leaflet or the inner leaflet can decrease the molecular density of the bilayer, making the remaining lipids in the bilayer have more space and freedom to reorganize themselves, thus can accelerate the flip-flop rate of the bilayer.

Besides, to see whether our results and conclusions drawn from pure water systems are also applicable to buffered systems, we have also investigated the interactions of CPZ with the dDSPC/DSPC and dDPPG/DPPG bilayers at the CPZ solution of pH = 7 (the pH was controlled by using 20 mM phosphate buffer solutions). Although there are differences in the measured flip-flop rates, the general trends are the same as compared to those without the phosphate buffer. That is, for the dDSPC/DSPC system, the higher the concentration of CPZ was, the faster the flip-flop rate of the bilayer occurred. For the dDPPG/DPPG bilayer, the addition of CPZ to the subphase to reach a low concentration of 0.1 mM immediately disordered the outer lipid leaflet, and the disordering of the inner leaflet was also faster at a higher CPZ concentration. These results demonstrated that our findings are also applicable to CPZ−bilayer interactions in buffer solutions (with constant pH value for CPZ solutions with different concentrations).

In biological membranes, the asymmetric distribution of phospholipids has profound implications in blood coagulation, cell clearance, membrane fusion, and apoptosis.[71] The lipid distribution is assisted by scramblase, a protein responsible for the translocation of phospholipids between the two leaflets of a lipid bilayer within a cell membrane. Our present work shows that CPZ can affect the lipid distribution by its detergent-like action through binding or solubilizing the lipid bilayer, which can significantly alter the properties and functions of the membrane and the membrane proteins embedded in the membranes.

Regarding the lipid components in biological cell membranes, PC is a key component of cell membranes which can account for almost 50% of the total lipids in cell membranes of animals and plants. It is commonly found in the exoplasmic or outer leaflet of a cell membrane. About 85% of the lipids found in lung surfactant are saturated PCs. PG is the main lipid component of some bacterial membranes, and it also exists in membranes of plants and animals with specific functions. In animal tissues, PG can be the second most abundant phospholipid in lung surfactant with up to 11% abundance. Moreover, the inner leaflet of the human red blood cell (RBC) plasma membrane bilayer contains virtually all of the anionic phospholipids[72,73] and is found to be able to sequester the positively charged CPZ via electrostatic attractive forces.[3] The above discussions show that both PC and PG are crucial cell membrane components and the interactions between CPZ and PC or PG bilayer should shed light on the understanding of CPZ's effects on various cellular functions.

With the help of an isotopically asymmetric lipid bilayer, we used SFG to examine how each individual leaflet of the lipid bilayer interacted with drug molecules and how the flip-flop process was affected by the drug. Especially, from the change of the flip-flop rate of lipids after the addition of drugs, important information on the drug−membrane interaction mechanism can be derived. For water-soluble drugs such as CPZ, the time-dependent SFG signals provide us information on the interaction kinetics between the drug and the lipid bilayer. For hydrophobic drugs with low water solubility which will be investigated in the future, we can construct an asymmetric lipid bilayer with a deuterated inner leaflet and an outer leaflet with a mixture of hydrogenated lipid and the hydrophobic drug. Such a lipid bilayer serves as a model to study how the hydrophobic drug molecules interact with the lipid bilayer after adsorbed to the outer leaflet. Also, by dissolving these hydrophobic drugs in an organic solvent such as dimethyl sulfoxide (DMSO), the above strategy to study water-soluble drugs can also be applied.

4. CONCLUSION

In this research we demonstrated that SFG spectroscopic results can help understand the molecular level interactions between the phenothiazine-type antipsychotic drug CPZ and model cell membranes. Although the effects of CPZ on PC and PG bilayers were both observed to be concentration dependent, the interaction mechanisms were different. For the PC bilayer, when the solution concentration of CPZ in the subphase was higher than 0.2 mM, CPZ behaved like a synthetic translocase or flippase that significantly accelerated the transbilayer movement of the lipid molecules. For PG, even at a low concentration of 0.1 mM, CPZ immediately disordered the outer leaflet of the DPPG bilayer and can then gradually reduce the ordering of the inner leaflet. The association of CPZ to the membrane surface can be verified by the change in the SFG spectra of the OH stretching vibrations of the interfacial water molecules. ATR-FTIR results revealed that the addition of CPZ to the subphase did not have significant effect on the dDSPC/dDSPC bilayer, especially at low CPZ concentrations (<2.0 mM). On the contrary, CPZ molecules could cause gel-to-fluid phase transition of the dDPPG/dDPPG bilayer at low CPZ concentrations below 2.0 mM. Higher CPZ concentration could lead to the dissolution of the dDPPG/dDPPG bilayer. In summary, the present work demonstrates that SFG is a powerful in situ and label-free technique to study drug−cell membrane interactions.

AUTHOR INFORMATION

Corresponding Authors

*E-mail: zhanc@umich.edu (Z.C.)
*E-mail: wufg@seu.edu.cn (F.-G.W.).

Notes

The authors declare no competing financial interest.

ACKNOWLEDGMENTS

This work was supported by grants from the Natural Science Foundation of China (21303017), the Natural Science Foundation of Jiangsu Province (KB20130601), and a project funded by the Priority Academic Program Development of Jiangsu Higher Education Institutions (1107037001). We also thank the support from the University of Michigan and the financial aids from Southeast University and the State Key Laboratory of Bioelectronics (Southeast University). We are also grateful for the helpful discussions with Bolin Li and Dr. Xiaolin Lu.

REFERENCES

(1) Seydel, J. K.; Coats, E. A.; Cordes, H. P.; Wiese, M. Drug Membrane Interaction and the Importance for Drug Transport, Distribution, Accumulation, Efficacy and Resistance. *Arch. Pharm.* **1994**, *327*, 601−610.

(2) Housley, G.; Born, G. V.; Conroy, D. M.; Berlin, D. M. J.; Smith, A. D. Influence of Dietary Lipids on the Effect of Chlorpromazine on Membrane Properties of Rabbit Red Cells. *Proc. R. Soc. London, B Biol. Sci.* **1986**, *227*, 43−51.

(3) Sheetz, M. P.; Singer, S. J. Biological Membranes as Bilayer Couples. A Molecular Mechanism of Drug-Erythrocyte Interactions. *Proc. Natl. Acad. Sci. U.S.A.* **1974**, *71*, 4457−4461.

(4) Brindley, D. N.; Bowley, M. Drugs Affecting the Synthesis of Glycerides and Phospholipids in Rat Liver. The Effects of Clofibrate, Halofenate, Fenfluramine, Amphetamine, Cinchocaine, Chlorpromazine, Demethylimipramine, Mepyramine and Some of Their Derivatives. *J. Biochem.* **1975**, *148*, 461−469.

(5) Nerdal, W.; Gundersen, S. A.; Thorsen, V.; Høiland, H.; Holmsen, H. Chlorpromazine Interaction with Glycerophospholipid Liposomes Studied by Magic Angle Spinning Solid State 13C-NMR and Differential Scanning Calorimetry. *Biochim. Biophys. Acta* **2000**, *1464*, 165−175.

(6) Jutila, A.; Söderlund, T.; Pakkanen, A. L.; Huttunen, M.; Kinnunen, P. K. J. Comparison of the Effects of Clozapine, Chlorpromazine, and Haloperidol on Membrane Lateral Heterogeneity. *Chem. Phys. Lipids* **2001**, *112*, 151−163.

(7) Agasøsler, A. V.; Tungodden, L. M.; Čějka, D.; Bakstad, E.; Sydnes, L. K.; Holmsen, H. Chorpromazine-Induced Increase in Dipalmitoylphosphatidylserine Surface Area in Monolayers at Room Temperature. *Biochem. Pharmacol.* **2001**, *61*, 817−825.

(8) Agasøsler, A. V.; Holmsen, H. Chlorpromazine Associates with Phosphatidylserines to Cause an Increase in the Lipid's Own Interfacial Molecular Area−Role of the Fatty Acyl Composition. *Biophys. Chem.* **2001**, *91*, 37−47.

(9) Chen, J. Y.; Brunauer, L. S.; Chu, F. C.; Helsel, C. M.; Gedde, M. M.; Huestis, W. H. Selective Amphipathic Nature of Chlorpromazine Binding to Plasma Membrane Bilayers. *Biochim. Biophys. Acta* **2003**, *1616*, 95−105.

(10) Girder, A. U.; Holmsen, H.; Nerdal, W. Chlorpromazine Interaction with Phosphatidylserines: A 13C and 31P Solid-State NMR Study. *Biochim. Biophys. Acta* **2004**, *1682*, 28−37.

(11) Wisniewska, A.; Wolnicka-Glubisz, A. ESR Studies on the Effect of Cholesterol on Chlorpromazine Interaction with Saturated and Unsaturated Liposome Membranes. *Biophys. Chem.* **2004**, *111*, 43−52.

(12) Hidalgo, A. A.; Caetano, W.; Tabak, M.; Oliveira, O. N., Jr. Interaction of Two Phenothiazine Derivatives with Phospholipid Monolayers. *Biophys. Chem.* **2004**, *109*, 85−104.

(13) Hidalgo, A. A.; Pimentel, A. S.; Tabak, M.; Oliveira, O. N., Jr. Thermodynamic and Infrared Analyses of the Interaction of Chlorpromazine with Phospholipid Monolayers. *J. Phys. Chem. B* **2006**, *110*, 19637−19646.

(14) Zhang, L. X.; Liu, J. Y.; Wang, E. K. A New Method for Studying the Interaction between Chlorpromazine and Phospholipid Bilayer. *Biochem. Biophys. Res. Commun.* **2008**, *373*, 202−205.

(15) Kitamura, K.; Takenaka, M.; Yoshida, S.; Ito, M.; Nakamura, Y.; Hozumi, K. Determination of Dissociation Constants of Sparingly Soluble Phenothiazine Derivatives by Second-Derivative Spectrophotometry. *Anal. Chim. Acta* **1991**, *242*, 131−135.

(16) Pickholz, M.; Oliveira, O. N., Jr.; Skaf, M. S. Interactions of Chlorpromazine with Phospholipid Monolayers: Effects of the Ionization State of the Drug. *Biophys. Chem.* **2007**, *125*, 425−434.

(17) Takegami, S.; Kitamura, K.; Kitade, T.; Hasegawa, K.; Nishihira, A. Effects of Particle Size and Cholesterol Content on the Partition Coefficients of Chlorpromazine and Triflupromazine between Phosphatidylcholine−Cholesterol Bilayers of Unilamellar Vesicles

and Water Studied by Second-Derivative Spectrophotometry. *J. Colloid Interface Sci.* **1999**, *220*, 81−87.
(18) Martins, P. T.; Velazquez-Campoy, A.; Vaz, W. L.; Cardoso, R. M.; Valério, J.; Moreno, M. J. Kinetics and Thermodynamics of Chlorpromazine Interaction with Lipid Bilayers: Effect of Charge and Cholesterol. *J. Am. Chem. Soc.* **2012**, *134*, 4184−4195.
(19) Pickholz, M.; Oliveira, O. N., Jr.; Skaf, M. S. Molecular Dynamics Simulations of Neutral Chlorpromazine in Zwitterionic Phospholipid Monolayers. *J. Phys. Chem. B* **2006**, *110*, 8804−8814.
(20) Nussio, M. R.; Liddell, M.; Sykes, M. J.; Miners, J. O.; Shapter, J. G. Dynamics of Phospholipid Membrane Growth and Drug-Membrane Interactions Probed by Atomic Force Microscopy. *J. Scanning Probe Microsc.* **2007**, *2*, 41−45.
(21) Nussio, M. R.; Sykes, M. J.; Miners, J. O.; Shapter, J. G. Kinetics Membrane Disruption Due to Drug Interactions of Chlorpromazine Hydrochloride. *Langmuir* **2009**, *25*, 1086−1090.
(22) Hendrich, A. B.; Michalak, K.; Wesołowska, O. Phase Separation Is Induced by Phenothiazine Derivatives in Phospholipid/Sphingomyelin/Cholesterol Mixtures Containing Low Levels of Cholesterol and Sphingomyelin. *Biophys. Chem.* **2007**, *130*, 32−40.
(23) Tessier, C.; Nuss, P.; Staneva, G.; Wolf, C. Modification of Membrane Heterogeneity by Antipsychotic Drugs: An X-ray Diffraction Comparative Study. *J. Colloid Interface Sci.* **2008**, *320*, 469−475.
(24) Wesołowska, O.; Michalak, K.; Hendrich, A. B. Direct Visualization of Phase Separation Induced by Phenothiazine-Type Antipsychotic Drugs in Model Lipid Membranes. *Mol. Membr. Biol.* **2011**, *28*, 103−114.
(25) Nguyen, T. T.; Rembert, K.; Conboy, J. C. Label-Free Detection of Drug-Membrane Association Using Ultraviolet−Visible Sum-Frequency Generation. *J. Am. Chem. Soc.* **2009**, *131*, 1401−1403.
(26) Nguyen, T. T.; Conboy, J. C. High-Throughput Screening of Drug−Lipid Membrane Interactions via Counter-Propagating Second Harmonic Generation Imaging. *Anal. Chem.* **2011**, *83*, 5979−5988.
(27) Shen, Y. R. *The Principles of Nonlinear Optics*; Wiley: New York, 1984.
(28) Perry, A.; Neipert, C.; Space, B.; Moore, P. B. Theoretical Modeling of Interface Specific Vibrational Spectroscopy: Methods and Applications to Aqueous Interfaces. *Chem. Rev.* **2006**, *106*, 1234−1258.
(29) Liljeblad, J. F. D.; Bulone, V.; Tyrode, E.; Rutland, M. W.; Johnson, C. M. Phospholipid Monolayers Probed by Vibrational Sum Frequency Spectroscopy: Instability of Unsaturated Phospholipids. *Biophys. J.* **2010**, *98*, L50−L52.
(30) Liljeblad, J. F. D.; Bulone, V.; Rutland, M. W.; Johnson, C. M. Supported Phospholipid Monolayers. The Molecular Structure Investigated by Vibrational Sum Frequency Spectroscopy. *J. Phys. Chem. C* **2011**, *115*, 10617−10629.
(31) Wurpel, G. W. H.; Sovago, M.; Bonn, M. Sensitive Probing of DNA Binding to a Cationic Lipid Monolayer. *J. Am. Chem. Soc.* **2007**, *129*, 8420−8421.
(32) Campen, R. K.; Ngo, T. T. M.; Sovago, M.; Ruysschaert, J. M.; Bonn, M. Molecular Restructuring of Water and Lipids upon the Interaction of DNA with Lipid Monolayers. *J. Am. Chem. Soc.* **2010**, *132*, 8037−8047.
(33) Darwish, N.; Eggers, P. K.; Ciampi, S.; Tong, Y.; Ye, S.; Paddon-Row, M. N.; Gooding, J. J. Probing the Effect of the Solution Environment around Redox-Active Moieties Using Rigid Anthraquinone Terminated Molecular Rulers. *J. Am. Chem. Soc.* **2012**, *134*, 18401−18409.
(34) Chen, X. Y.; Wang, J.; Kristalyn, C. B.; Chen, Z. Real-Time Structural Investigation of a Lipid Bilayer during Its Interaction with Melittin Using Sum Frequency Generation Vibrational Spectroscopy. *Biophys. J.* **2007**, *93*, 866−875.
(35) Tong, Y.; Li, N.; Liu, H.; Ge, A.; Osawa, M.; Ye, S. Mechanistic Studies by Sum-Frequency Generation Spectroscopy: Hydrolysis of a Supported Phospholipid Bilayer by Phospholipase A2. *Angew. Chem., Int. Ed.* **2010**, *49*, 2319−2323.
(36) Chen, X.; Hua, W.; Huang, Z.; Allen, H. C. Interfacial Water Structure Associated with Phospholipid Membranes Studied by Phase-Sensitive Vibrational Sum Frequency Generation Spectroscopy. *J. Am. Chem. Soc.* **2010**, *132*, 11336−11342.
(37) Fu, L.; Ma, G.; Yan, E. C. In Situ Misfolding of Human Islet Amyloid Polypeptide at Interfaces Probed by Vibrational Sum Frequency Generation. *J. Am. Chem. Soc.* **2010**, *132*, 5405−5412.
(38) Fu, L.; Liu, J.; Yan, E. C. Chiral Sum Frequency Generation Spectroscopy for Characterizing Protein Secondary Structures at Interfaces. *J. Am. Chem. Soc.* **2011**, *133*, 8094−8097.
(39) Watry, M. R.; Tarbuck, T. L.; Richmond, G. L. Vibrational Sum-Frequency Studies of a Series of Phospholipid Monolayers and the Associated Water Structure at the Vapor/Water Interface. *J. Phys. Chem. B* **2003**, *107*, 512−518.
(40) Zhang, Z.; Guo, Y.; Lu, Z.; Velarde, L.; Wang, H. F. Resolving Two Closely Overlapping−CN Vibrations and Structure in the Langmuir Monolayer of the Long-Chain Nonadecanenitrile by Polarization Sum Frequency Generation Vibrational Spectroscopy. *J. Phys. Chem. C* **2012**, *116*, 2976−2987.
(41) Mondal, J. A.; Nihonyanagi, S.; Yamaguchi, S.; Tahara, T. Three Distinct Water Structures at a Zwitterionic Lipid/Water Interface Revealed by Heterodyne-Detected Vibrational Sum Frequency Generation. *J. Am. Chem. Soc.* **2012**, *134*, 7842−7850.
(42) Mondal, J. A.; Nihonyanagi, S.; Yamaguchi, S.; Tahara, T. Structure and Orientation of Water at Charged Lipid Monolayer/Water Interfaces Probed by Heterodyne-Detected Vibrational Sum Frequency Generation Spectroscopy. *J. Am. Chem. Soc.* **2010**, *132*, 10656−10657.
(43) Ye, S. J.; Li, H. C.; Yang, W. L.; Luo, Y. Accurate Determination of Interfacial Protein Secondary Structure by Combining Interfacial-Sensitive Amide I and Amide III Spectral Signals. *J. Am. Chem. Soc.* **2014**, *136*, 1206−1209.
(44) Ma, S. L.; Li, H. C.; Tian, K. Z.; Ye, S. J.; Luo, Y. In Situ and Real Time SFG Measurements Reveal Organization and Transport of Cholesterol Analog 6-Ketocholestanol in Cell Membrane. *J. Phys. Chem. Lett.* **2014**, *5*, 419−424.
(45) Wei, F.; Li, H. C.; Ye, S. J. Specific Ion Interaction Dominates over Hydrophobic Matching Effects in Peptide-Lipid Bilayer Interactions: The Case of Short Peptide. *J. Phys. Chem. C* **2013**, *117*, 26190−26196.
(46) Ye, S. J.; Li, H. C.; Wei, F.; Jasensky, J.; Boughton, A. P.; Yang, P.; Chen, Z. Observing a Model Ion Channel Gating Action in Model Cell Membranes in Real Time in Situ: Membrane Potential Change Induced Alamethicin Orientation Change. *J. Am. Chem. Soc.* **2012**, *134*, 6237−6243.
(47) Yang, P.; Wu, F. G.; Chen, Z. Dependence of Alamethicin Membrane Orientation on the Solution Concentration. *J. Phys. Chem. C* **2013**, *117*, 3358−3365.
(48) Yang, P.; Wu, F. G.; Chen, Z. Lipid Fluid−Gel Phase Transition Induced Alamethicin Orientational Change Probed by Sum Frequency Generation Vibrational Spectroscopy. *J. Phys. Chem. C* **2013**, *117*, 17039−17049.
(49) Anglin, T. C.; Conboy, J. C. Lateral Pressure Dependence of the Phospholipid Transmembrane Diffusion Rate in Planar-Supported Lipid Bilayers. *Biophys. J.* **2008**, *95*, 186−193.
(50) Anglin, T. C.; Conboy, J. C. Kinetics and Thermodynamics of Flip-Flop in Binary Phospholipid Membranes Measured by Sum-Frequency Vibrational Spectroscopy. *Biochemistry* **2009**, *48*, 10220−10234.
(51) Liu, J.; Brown, K. L.; Conboy, J. C. The Effect of Cholesterol on the Intrinsic Rate of Lipid Flip-Flop as Measured by Sum-Frequency Vibrational Spectroscopy. *Faraday Discuss.* **2013**, *161*, 45−61.
(52) Liu, J.; Conboy, J. C. Direct Measurement of the Transbilayer Movement of Phospholipids by Sum-Frequency Vibrational Spectroscopy. *J. Am. Chem. Soc.* **2004**, *126*, 8376−8377.
(53) Liu, J.; Conboy, J. C. 1,2-Diacyl-Phosphatidylcholine Flip-Flop Measured Directly by Sum-Frequency Vibrational Spectroscopy. *Biophys. J.* **2005**, *89*, 2522−2532.
(54) Anglin, T. C.; Cooper, M. P.; Li, H.; Chandler, K.; Conboy, J. C. Free Energy and Entropy of Activation for Phospholipid Flip-Flop in

Planar Supported Lipid Bilayers. *J. Phys. Chem. B* **2010**, *114*, 1903−1914.
(55) Kuroda, Y.; Kitamura, K. Intra- and intermolecular proton-proton nuclear Overhauser effect studies on the interactions of chlorpromazine with lecithin vesicles. *J. Am. Chem. Soc.* **1984**, *106*, 1−6.
(56) Verreault, D.; Hua, W.; Allen, H. C. From Conventional to Phase-Sensitive Vibrational Sum Frequency Generation Spectroscopy: Probing Water Organization at Aqueous Interfaces. *J. Phys. Chem. Lett.* **2012**, *3*, 3012−3028.
(57) Ong, S. W.; Zhao, X. L.; Eisenthal, K. B. Polarization of Water Molecules at a Charged Interface: Second Harmonic Studies of the Silica/Water Interface. *Chem. Phys. Lett.* **1992**, *191*, 327−335.
(58) Zhao, X. L.; Ong, S. W.; Eisenthal, K. B. Polarization of Water Molecules at a Charged Interface. Second Harmonic Studies of Charged Monolayers at the Air/Water Interface. *Chem. Phys. Lett.* **1993**, *202*, 513−520.
(59) Sung, W.; Seok, S.; Kim, D.; Tian, C. S.; Shen, Y. R. Sum-Frequency Spectroscopic Study of Langmuir Monolayers of Lipids Having Oppositely Charged Headgroups. *Langmuir* **2010**, *26*, 18266−18272.
(60) Wei, X.; Miranda, P. B.; Zhang, C.; Shen, Y. R. Sum-Frequency Spectroscopic Studies of Ice Interfaces. *Phys. Rev. B* **2002**, *66*, 085401/1−085401/13.
(61) Du, Q.; Superfine, R.; Freysz, E.; Shen, Y. R. Vibrational Spectroscopy of Water at the Vapor/Water Interface. *Phys. Rev. Lett.* **1993**, *70*, 2313−2316.
(62) Broniec, A.; Gjerde, A. U.; Ølmheim, A. B.; Holmsen, H. Trifluoperazine Causes a Disturbance in Glycerophospholipid Monolayers Containing Phosphatidylserine (PS): Effects of pH, Acyl Unsaturation, and Proportion of PS. *Langmuir* **2007**, *23*, 694−699.
(63) Steinkopf, S.; Simeunović, A.; Bustad, H. J.; Ngo, T. H.; Sveaass, H.; Gjerde, A. U.; Holmsen, H. pH-Dependent Interaction of Psychotropic Drug with Glycerophospholipid Monolayers Studied by the Langmuir Technique. *Biophys. Chem.* **2010**, *152*, 65−73.
(64) Chen, S.; Gjerde, A. U.; Holmsen, H.; Nerdal, W. Importance of Polyunsaturated Acyl Chains in Chlorpromazine Interaction with Phosphatidylserines: A 13C and 31P Solid-State NMR Study. *Biophys. Chem.* **2005**, *117*, 101−109.
(65) Song, C.; Holmsen, H.; Nerdal, W. Existence of Lipid Microdomains in Bilayer of Dipalmitoyl Phosphatidylcholine (DPPC) and 1-Stearoyl-2-docosahexenoyl Phosphatidylserine (SDPS) and Their Perturbation by Chlorpromazine: A ^{13}C and ^{31}P Solid-State NMR Study. *Biophys. Chem.* **2006**, *120*, 178−187.
(66) Rosso, J.; Zachowski, A.; Devaux, P. F. Influence of Chlorpromazine on the Transverse Mobility of Phospholipids in the Human Erythrocyte Membrane: Relation to Shape Changes. *Biochim. Biophys. Acta* **1988**, *942*, 271−279.
(67) Schrier, S. L.; Zachowski, A.; Devaux, P. F. Mechanisms of Amphipath-Induced Stomatocytosis in Human Erythrocytes. *Blood* **1992**, *79*, 782−786.
(68) Ahyayauch, H.; Bennouna, M.; Alonso, A.; Goni, F. M. Detergent Effects on Membranes at Subsolubilizing Concentrations: Transmembrane Lipid Motion, Bilayer Permeabilization, and Vesicle Lysis/Reassembly Are Independent Phenomena. *Langmuir* **2010**, *26*, 7307−7313.
(69) Wu, F. G.; Yu, J. S.; Sun, S. F.; Yu, Z. W. Comparative Studies on the Crystalline to Fluid Phase Transitions of Two Equimolar Cationic/Anionic Surfactant Mixtures Containing Dodecylsulfonate and Dodecylsulfate. *Langmuir* **2011**, *27*, 14740−14747.
(70) Pabst, G.; Grage, S. L.; Danner-Pongratz, S.; Jing, W.; Ulrich, A. S.; Watts, A.; Lohner, K.; Hickel, A. Membrane Thickening by the Antimicrobial Peptide PGLa. *Biophys. J.* **2008**, *95*, 5779−5788.
(71) Schlegel, R. A.; Williamson, P. Phosphatidylserine, a Death Knell. *Cell Death Differ.* **2001**, *8*, 551−563.
(72) Bretscher, M. S. Asymmetrical Lipid Bilayer Structure for Biological Membranes. *Nat. New Biol.* **1972**, *236*, 11−12.
(73) Verkleij, A. J.; Zwaal, R. F. A.; Roelofsen, B.; Comfurius, P.; Kastelijn, D.; Van Deenen, L. L. M. The Asymmetric Distribution of Phospholipids in the Human Red Cell Membrane. A Combined Study Using Phospholipases and Freeze-Etch Electron Microscopy. *Biochim. Biophys. Acta* **1973**, *323*, 178−193.